

Figure S1. TBT does not attenuate osteogenic differentiation, but results in persistent expression of adipose lineage markers (Related to Figure 1). (A) Mouse MSCs were pretreated with vehicle control (DMSO), ROSI (10, 100 nM), 4204 (10, 100 nM), or TBT (5, 50 nM) and then differentiated for 2 weeks with adipose induction cocktail. RNA from mouse MSCs subjected to a commitment assay was collected at Day 14 and analyzed for markers of the adipose differentiation. (B-D) MSCs were pretreated for 48 hours with DMSO, ROSI (10, 100 nM), 4204 (10, 100 nM), or TBT (5, 50 nM) and then differentiated towards the bone lineage with an osteogenic induction cocktail. RNA was collected at Day 0 (B) and Day 14 (C-D) for gene expression analysis by QPCR. (B) RNA from Day 0 was analyzed for expression of genes involved in MSC lineage commitment. (C-D) Gene expression of osteogenic (C) and adipogenic (D) gene markers at Day 14. Data are represented as mean \pm SEM. 1-way ANOVA, Dunnett's test, * $P < 0.05$, ** $P < 0.01$, *** $P < 0.001$.

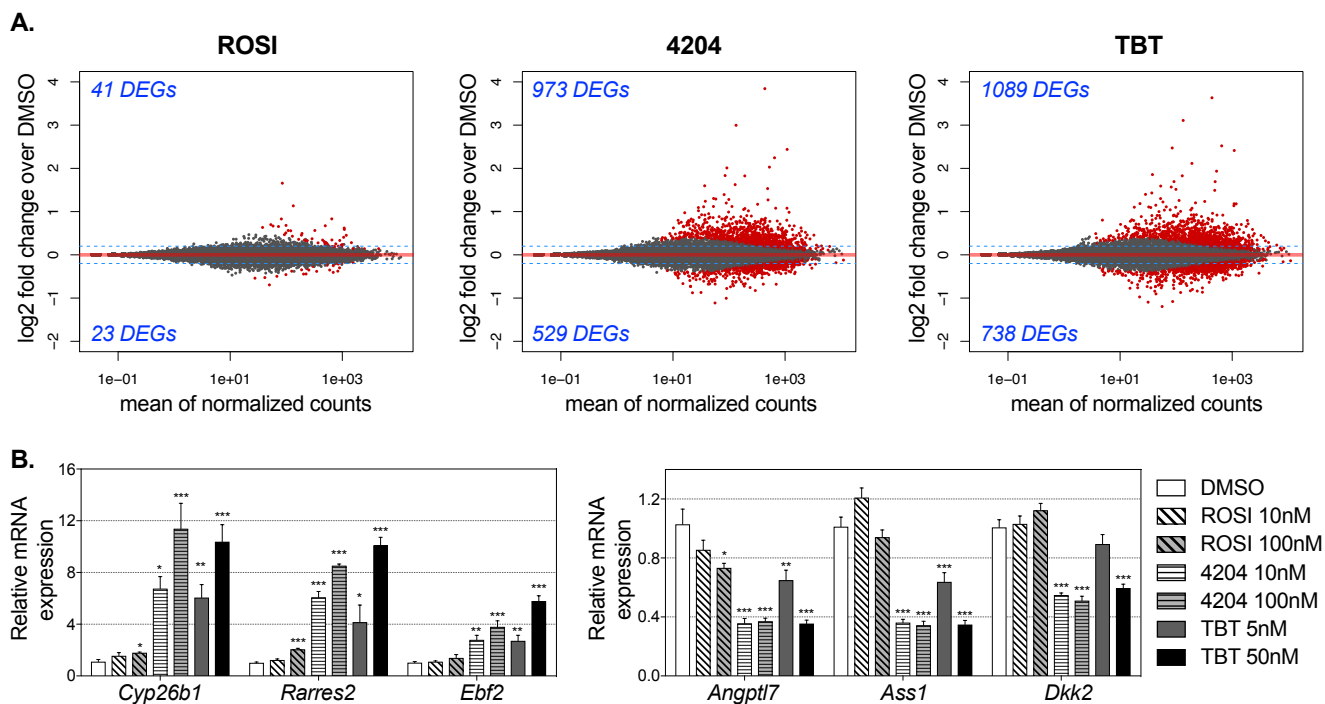


Figure S2. Genome-wide expression changes in undifferentiated MSCs exposed to TBT, 4204, ROSI, or DMSO control (Related to Figure 5). (A) MA-plots of expression changes for each treatment over vehicle control. The total number of up- and down-regulated differentially expressed genes (DEGs) (adjusted p-value <0.01, red dots; absolute value[log₂ fold change] >0.2, blue dotted lines) are indicated in blue text. (B) RNA from Day 0 pretreated MSCs was analyzed for expression of novel RXR target genes identified in RNA-Seq data. Data are represented as mean ± SEM. 1-way ANOVA, Dunnett's test, * P < 0.05, ** P < 0.01, *** P < 0.001.

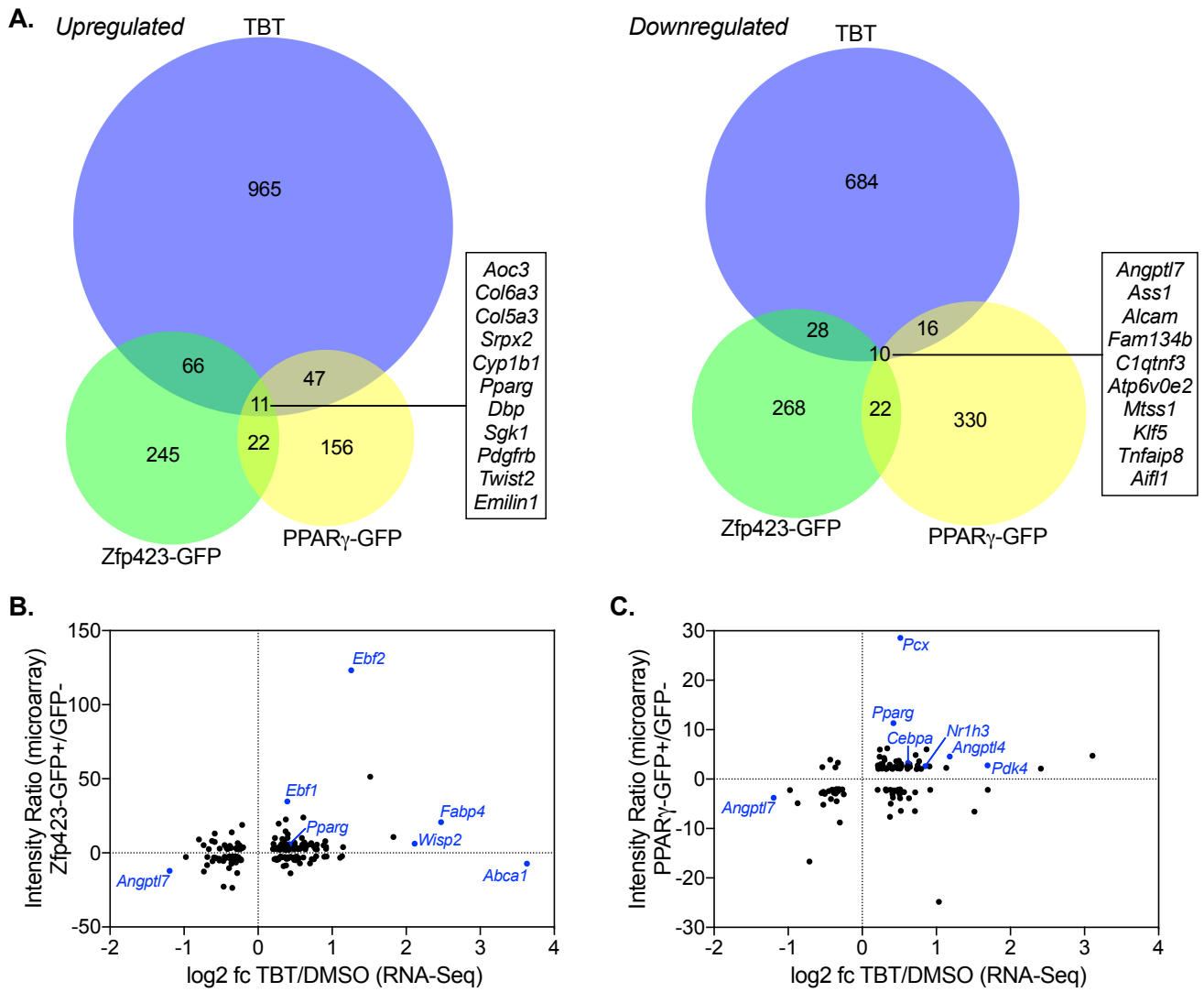


Figure S3. TBT targets genes that define the preadipocyte *in vivo* (Related to Figure 5). Genes differentially expressed in TBT-exposed MSCs were compared with previous microarray studies of adipose progenitors *in vivo*. (A) Genes up and downregulated by TBT were compared with the expression profile of Zfp423+ and PPAR γ + gonadal adipose tissue SVF. (B, C) Comparison of genes differentially expressed in TBT and (B) Zfp423+ or (C) PPAR γ + SVF.

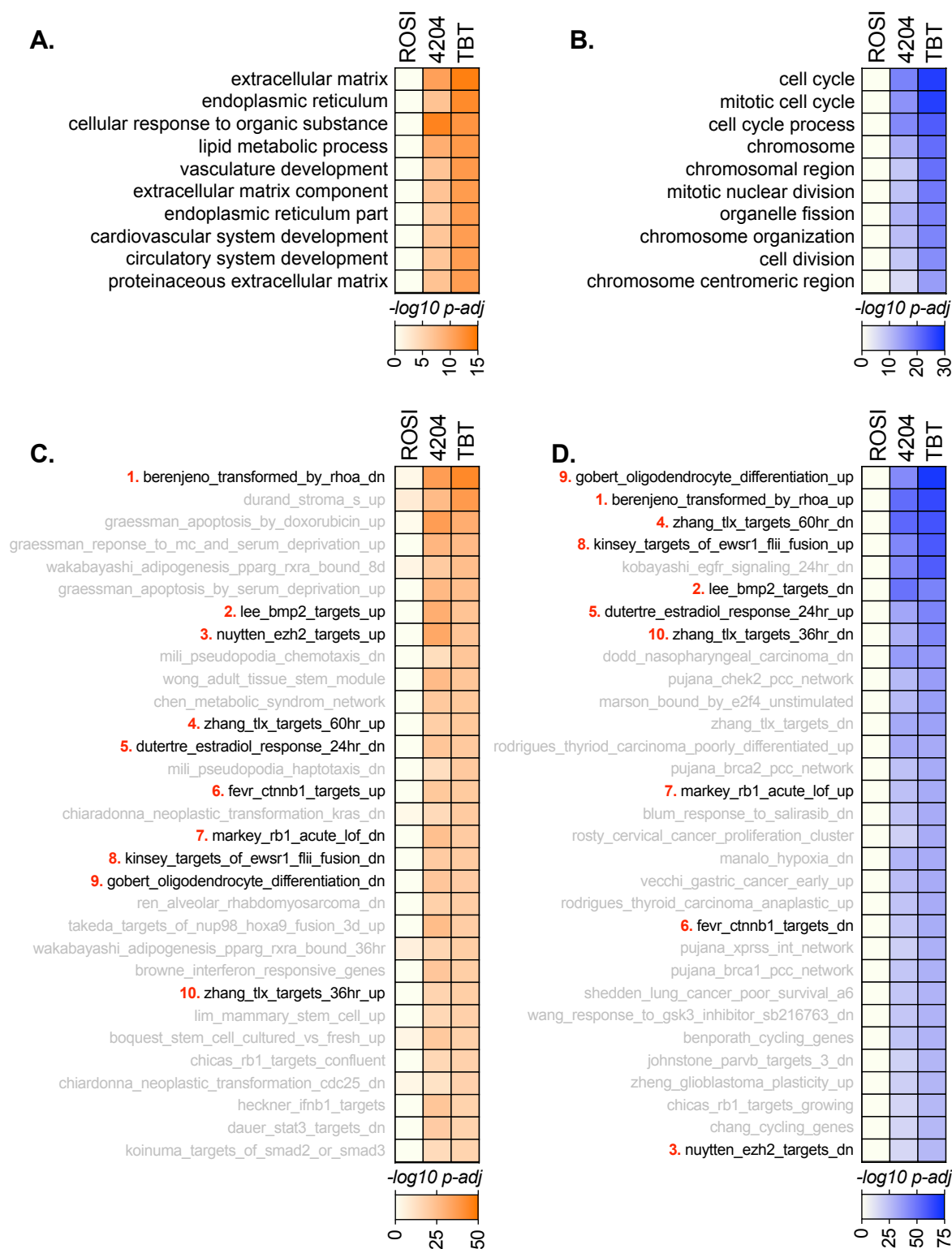


Figure S4. Gene ontology and pathway analysis of TBT-exposed MSCs (Related to Figure 5). GO term and pathway analysis was conducted using the Molecular Signaling Database (MSigDB, Broad Institute) curated gene sets on genes altered by TBT, 4204, and ROSI. Differentially expressed genes were analyzed for enrichment in GO terms and pathways by hypergeometric test; enriched gene sets were ranked by adjusted p-value (Benjamini-Hochberg). (A, B) Top GO terms enriched in genes (A) upregulated and (B) downregulated by TBT, with corresponding 4204 and ROSI. (C, D) Top MSigDB pathways enriched in genes (C) upregulated and (D) downregulated by TBT, with corresponding 4204 and ROSI enrichment. 10 pathways with corresponding, oppositely regulated gene sets are numbered in red.

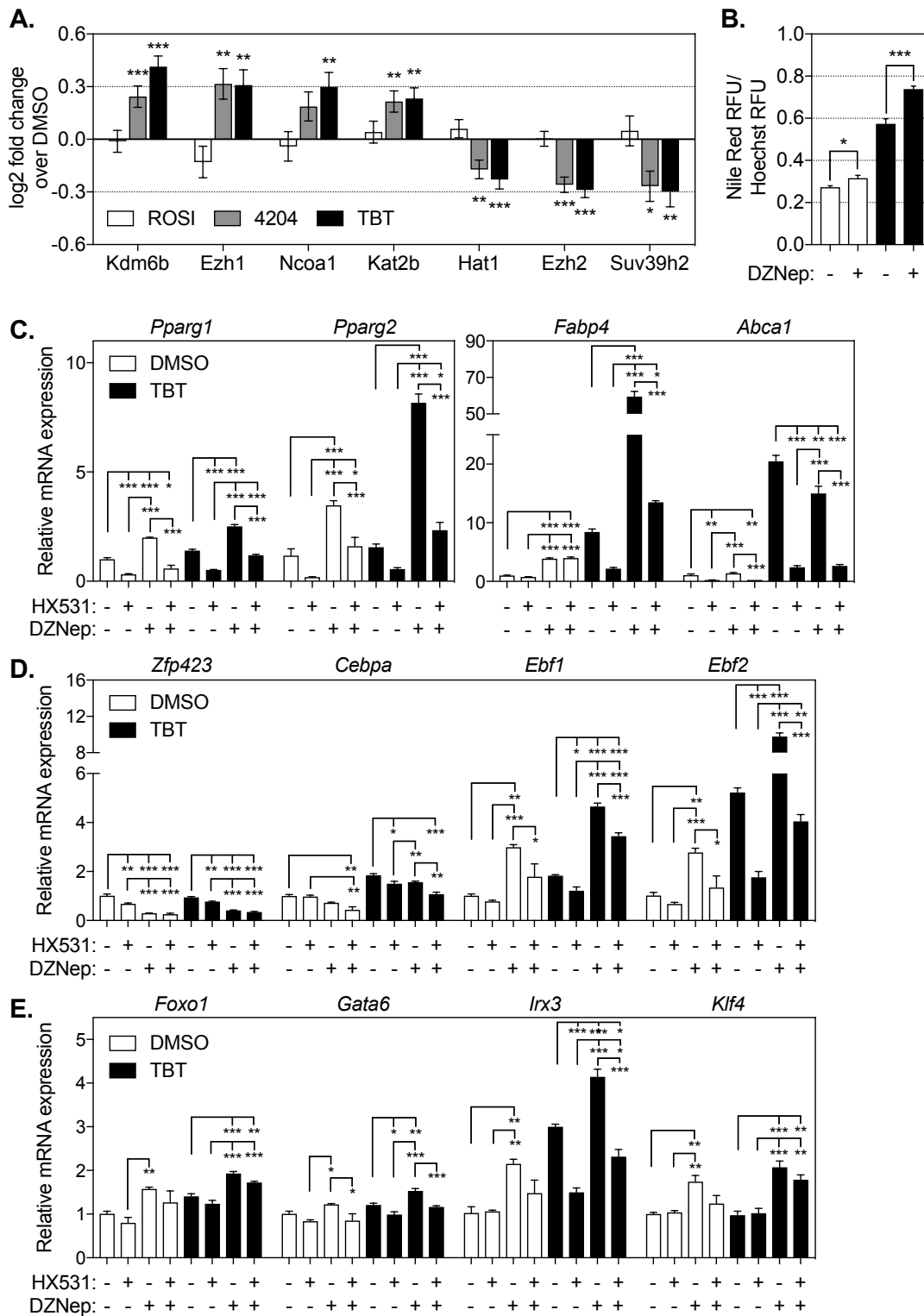


Figure S5. TBT acts through RXR to repress EZH2 and other histone modifying enzymes (Related to Figure 6). (A) All histone modifiers identified as DEGs by RNA-Seq. (B) MSCs were pretreated with vehicle control or TBT (50 nM) with and without the EZH2 inhibitor DZNep (1 uM), then differentiated into adipocytes and stained for lipid accumulation. Data are represented as mean \pm SEM. Student's t-test, * P < 0.05, ** P < 0.01, *** P < 0.001. (C-E) Day 0 gene expression following chemical pretreatment with vehicle control or TBT (50 nM), with or without the RXR inhibitor HX531 (10 uM) and/or DZNep (1 uM). Expression of (C-D) adipogenic markers and (E) genes in proximity to decreased H3K27me₃ differential islands was assessed. For each DMSO and TBT group, 1-way ANOVA, Tukey's test, * P < 0.05, ** P < 0.01, *** P < 0.001.

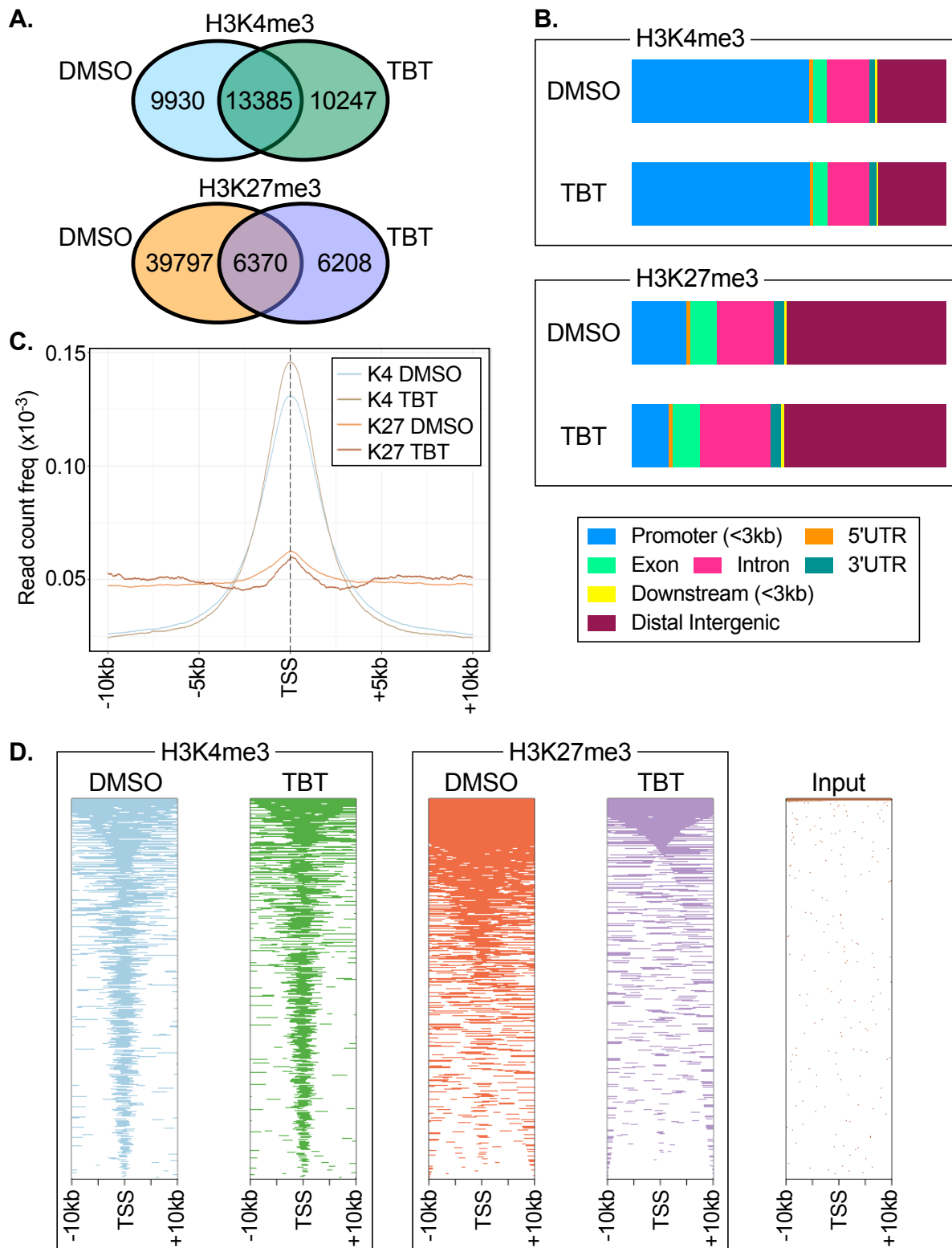


Figure S6. TBT the genome-wide distribution of H3K27me3 islands (Related to Figure 6). Chromatin from MSCs pretreated with vehicle control (DMSO) or TBT (50 nM) was immunoprecipitated for the histone marks H3K4me3 and H3K27me3 and subjected to library preparation and sequencing. Reads were aligned to the mouse genome (mm10), peaks/islands were called in SICER, and data was visualized in ChipSeeker (R/Bioconductor). (A) Overlaps of H3K4me3 and H3K27me3 peaks/islands from both treatment groups. (B) Genomic distribution, displayed as a percentage, of all H3K4me3 peaks and H3K27me3 islands. (C) Read count frequency of each histone mark and treatment 10 kb proximal and distal to the TSS. (D) Heatmap of ChIP signal for each histone mark, treatment, and input control around the TSS.

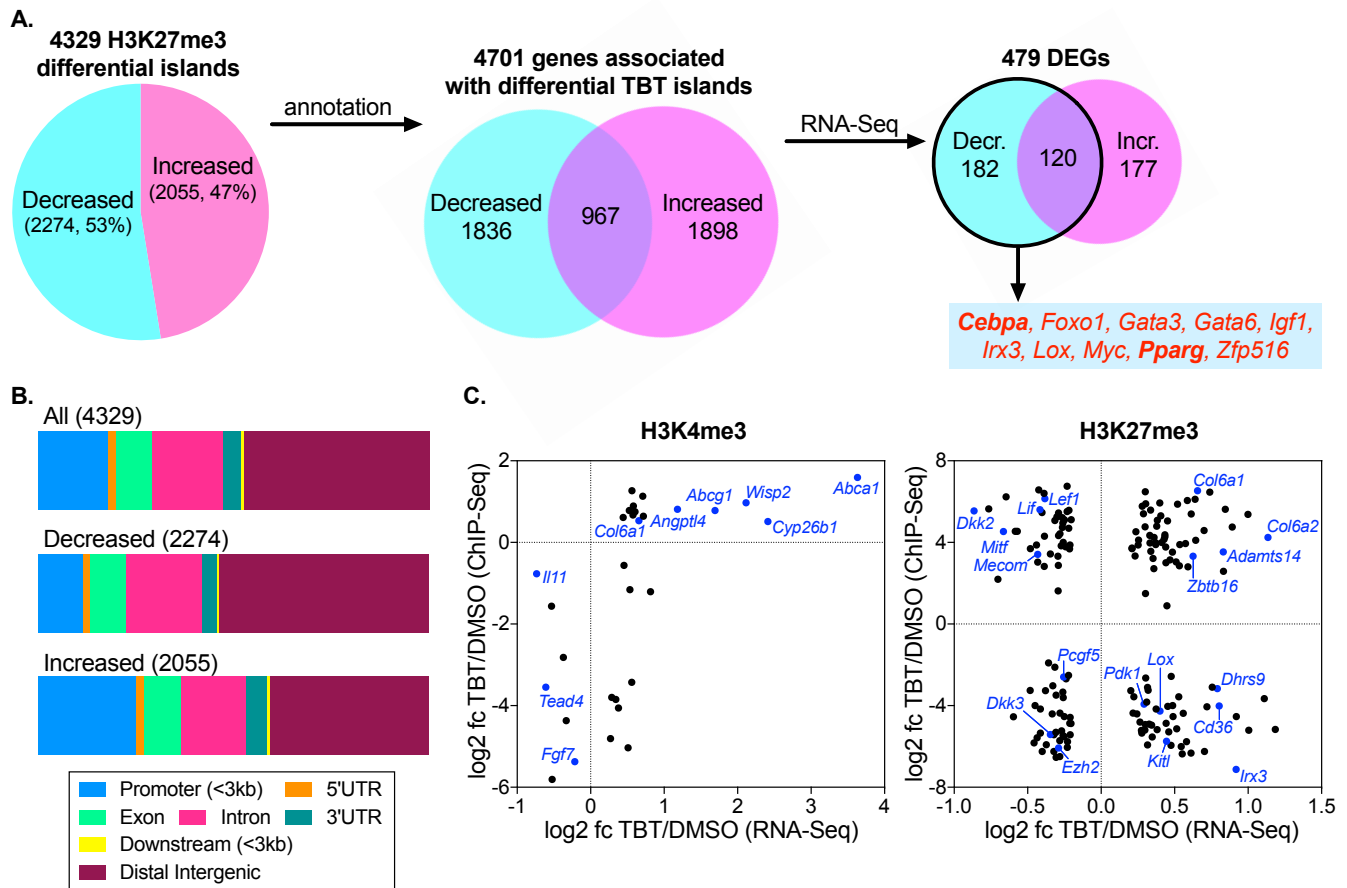


Figure S7. H3K27me3 differential islands are near differentially expressed genes that play critical roles in adipogenesis (Related to Figure 7). (A) All 4329 H3K27me3 differential islands were annotated to 4701 neighboring genes (< 1Mb) using GREAT. 479 of these genes were differentially expressed; up-regulated DEGs annotated by at least one decreased differential island are indicated in red. (B) Genome-wide distribution of all H3K27me3 differential islands, decreased islands, and increased islands. (C) DEGs with differential peaks/islands within promoters or gene bodies were identified. Gene-level correspondence between RNA expression and differential H3K4me3 (left panel) or H3K27me3 (right panel) ChIP signal.